

## New Developments of EPOS 2

T. Pierog

*KIT, Institut für Kernphysik, Karlsruhe, Germany*

Iu. Karpenko

*Bogolyubov Institute for Theoretical Physics, Kiev, Ukraine*

S. Porteboeuf

*University of Clermont-Ferrand, Clermont-Ferrand, France*

K. Werner

*SUBATECH, University of Nantes – IN2P3/CNRS– EMN, Nantes, France*

Since 2006, EPOS hadronic interaction model is being used for very high energy cosmic ray analysis. Designed for minimum bias particle physics and used to have a precise description of SPS and RHIC heavy ion collisions, EPOS brought more detailed description of hadronic interactions in air shower development. Thanks to this model it was possible to understand why there was less muons in air shower simulations than observed in real data. With the start of the LHC era, a better description of hard processes and collective effects is needed to understand deeply the incoming data. We will describe the basic physics in EPOS and the new developments and constraints which are taken into account in EPOS 2.

### 1. INTRODUCTION

Air shower simulations are a very powerful tool to interpret ground based cosmic ray experiments. However, most simulations are still based on hadronic interaction models being more than 10 years old. Much has been learned since, in particular due to new data available from the SPS and RHIC accelerators.

In this paper, we discuss the new development of the EPOS model, the latter one being a hadronic interaction model, which does very well compared to RHIC data [1], and also other particle physics experiments (especially SPS experiments at CERN). Used for air shower analysis since 2006, the last version 1.99 released in 2009 gives very interesting results in term of mass composition [2]. Due to the constraints of particle physics, air shower simulations using EPOS present a larger number of muons at ground [3]. It allows for the first time to reproduce both the muon number and the elongation rate using a reasonable average mass for all energies between the knee and the Greisen-Zatsepin-Kuzmin (GZK) cut-off.

On the other hand, the new measurements at LHC give us the opportunity to test the model more deeply. After a general introduction of the EPOS model, we will explain in this paper, the new developments done in EPOS 2.

### 2. EPOS MODEL

One may consider the simple parton model to be the basis of high energy hadron-hadron interaction models, which can be seen as an exchange of a “parton ladder” between the two hadrons.

In EPOS, the term “parton ladder” is actually meant to contain two parts [4]: the hard one, as discussed

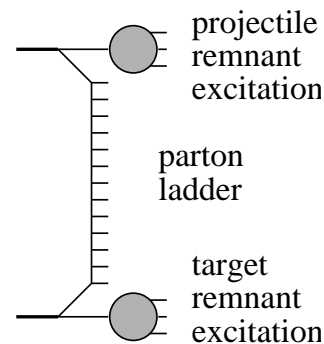


Figure 1: Elementary parton-parton scattering: the hard scattering in the middle is preceded by parton emissions attached to remnants. The remnants are an important source of particle production even at RHIC energies.

above, and a soft one, which is a purely phenomenological object, parameterized in Regge pole fashion.

In additions to the parton ladder, there is another source of particle production: the two off-shell remnants, see fig. 1. We showed in ref. [5] that this “three object picture” can solve the “multi-strange baryon problem” of conventional high energy models, see ref. [6].

Hence EPOS is a consistent quantum mechanical multiple scattering approach based on partons and strings [4], where cross sections and the particle production are calculated consistently, taking into account energy conservation in both cases (unlike other models where energy conservation is not considered for cross section calculations [7]). Nuclear effects related to Cronin transverse momentum broadening, parton saturation, and screening have been introduced into EPOS [8]. Furthermore, high density effects leading to collective behavior in heavy ion collisions are also taken into account [9].

Insert PSN Here

Thanks to a Monte Carlo, first the collision configuration is determined: i.e. the number of each type of Pomerons exchanged between the projectile and target is fixed and the initial energy is shared between the Pomerons and the two remnants. Then particle production is accounted from two kinds of sources, remnant decay and cut Pomeron. A Pomeron may be regarded as a two-layer (soft) parton ladder attached to projectile and target remnants through its two legs. Each leg is a color singlet, of type  $q\bar{q}$ ,  $qqq$  or  $\bar{q}\bar{q}\bar{q}$  from the sea, and then each cut Pomeron is regarded as two strings, Cf. fig. 2 a) and b).

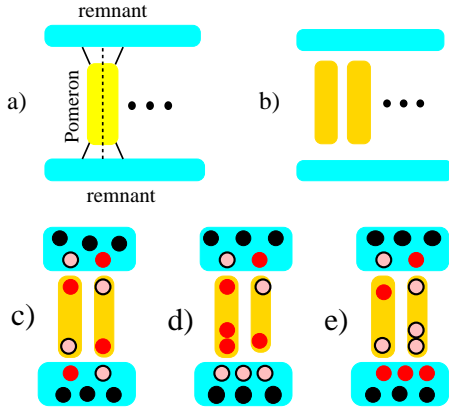


Figure 2: a) Each cut Pomeron is regarded as two strings b). c) The most simple and frequent collision configuration has two remnants and only one cut Pomeron represented by two  $q - \bar{q}$  strings. d) One of the  $\bar{q}$  string ends can be replaced by a  $qq$  string end. e) With the same probability, one of the  $q$  string ends can be replaced by a  $\bar{q}\bar{q}$  string end.

It is a natural idea to take quarks and anti-quarks from the sea as string ends for soft Pomeron in EPOS, because an arbitrary number of Pomerons may be involved.

Thus, besides the three valence quarks, each remnant has additionally quarks and anti-quarks to compensate the flavors of the string ends, as shown in fig. 2 c). According to its number of quarks and anti-quarks, to the phase space, and to an excitation probability, a remnant decays into mesons and/or (anti)baryons [5]. Furthermore, this process leads to a baryon stopping phenomenon in which the baryon number can be transferred from the remnant to the string ends (for instance in 2 d), depending on the process, the  $3\bar{q} + 3q$  can be seen as 3 mesons or a baryon-antibaryon pair).

In case of meson projectile, this kind of diquark pair production at the string ends leads to an increase of the (anti)baryon production in the forward production in agreement with low energy pion-nucleus data [10] as shown fig. 3. Comparing to QGSJETII model [11]

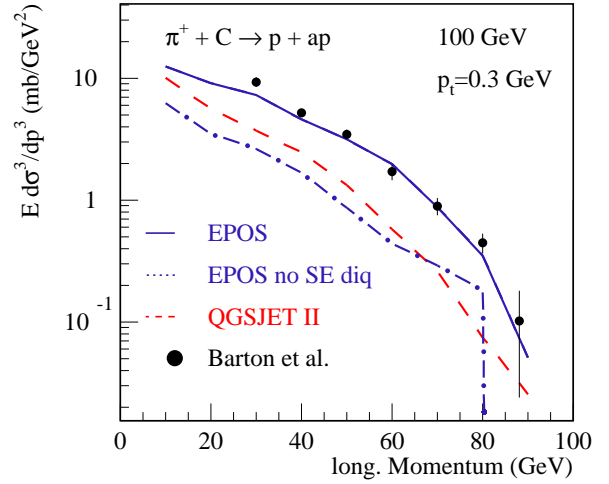


Figure 3: Model comparison: longitudinal momentum distributions of pion carbon collisions at 100 GeV from EPOS with (full) or without (dashed-dotted) sting-end diquarks and QGSJETII (dashed) compared to data [10].

which do not have diquark as string ends or using only  $q\bar{q}$  as string end in EPOS, we can clearly see that this process is needed to reproduce experimental data. As a consequence it is part of the larger number of muons in air shower simulations with EPOS.

Energy momentum sharing and remnant treatment are the key points of the model concerning air shower simulations because they directly influence the multiplicity and the inelasticity of the model.

### 3. NEW DEVELOPMENTS

With the start of the LHC era, it is now possible to develop some particular physics point of the EPOS model, which will be possible to test with newly available data.

#### 3.1. Hydrodynamical Evolution

In EPOS 2, a new tool has been developed for treating the hydrodynamical evolution (see [12] for details and tests with AuAu data).

As we saw, in case of elementary reactions like proton proton scattering (at moderately relativistic energies), hadron production is realized via string breaking, such that string fragments are identified with hadrons. When it comes to heavy ion collisions or very high energy proton-proton scattering, the procedure has to be modified, since the density of strings will be so high that they cannot possibly decay independently. For technical reasons, we split each string

into a sequence of string segments, at a given proper-time  $\tau_0$ , corresponding to widths  $\delta\alpha$  and  $\delta\beta$  in the string parameter space. One distinguishes between string segments in dense areas (more than some critical density  $\rho_0$  of segments per unit volume), from those in low density areas. The high density areas are referred to as core, the low density areas as corona [9]. String segments with large transverse momentum (close to a kink) are excluded from the core. Based on the four-momenta of infinitesimal string segments,

$$\delta p = \left\{ \frac{\partial X(\alpha, \beta)}{\partial \beta} \delta\alpha + \frac{\partial X(\alpha, \beta)}{\partial \alpha} \delta\beta \right\}, \quad (1)$$

one computes the energy-momentum tensor and conserved currents. The corresponding energy density  $\varepsilon(\tau_0, \vec{x})$  and the flow velocity  $\vec{v}(\tau_0, \vec{x})$  serve as initial conditions for the subsequent hydrodynamic evolutions, which is characterized by :

- consideration of the possibility to have a (moderate) initial collective transverse flow;
- event-by-event procedure, taking into the account the highly irregular space structure of single events, being experimentally visible via so-called ridge structures in two-particle correlations;
- use of an efficient code for solving the hydrodynamic equations in 3+1 dimensions, including the conservation of baryon number, strangeness, and electric charge;
- employment of a realistic equation-of-state, compatible with lattice gauge results – with a cross-over transition from the hadronic to the plasma phase;
- use of a complete hadron resonance table, making our calculations compatible with the results from statistical models;
- hadronic cascade procedure after hadronization from the thermal system at an early stage.

### 3.2. Diffraction

In order to produce hard diffractive events as measured at Tevatron and most likely at LHC in a near future, it was necessary to improve the way of producing diffractive events in EPOS 2. To get a consistent description of low mass and high mass diffraction, an effective diffractive Pomeron is used in addition to the soft and semi-hard Pomeron. This effective object represents in reality all type of diagrams (soft and hard component) which are not connected to at least one of the remnant, leaving the latter intact. The triple Pomeron would be part of this object, but all higher

orders too. Since this object is very difficult to calculate explicitly at all orders including proper energy conservation, we use a simple parameterization having the same form as the usual Pomeron (see [8]) and fixing the parameters using the proton-proton single diffractive cross section and the energy spectrum of leading protons.

### 3.3. Structure Function

In order to test hard scattering at LHC (or Tevatron) using EPOS, it is important to be able to reproduce the structure function  $F_2$  as measured thanks to the HERA electron-proton collider.

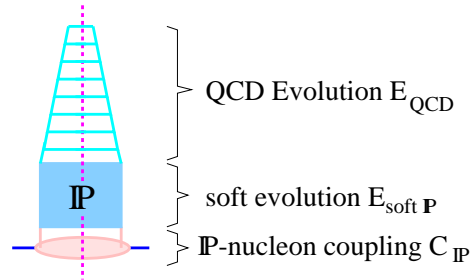


Figure 4: “Half-”Pomeron corresponding to the parton distribution function tested via the structure function  $F_2$ .

In EPOS,  $F_2$  corresponds to a “half” hard or semi-hard Pomeron as illustrated on fig. 4. The cross section of a quark with a given  $Q^2$  as a function of the momentum fraction  $x$  can be calculated using the convolution of a soft pre-evolution with the DGLAP equations for the perturbative development of the parton ladder [4]. Taking into account the effective corrections due to higher order diagrams in the connection between the Pomeron and the nucleon (and fixed with proton-proton cross section), we obtain the structure function as shown on fig. 5.

### 3.4. Baryon production

In EPOS 2, not only the soft Pomerons can have a diquark as string-end, but the semi-hard Pomerons are now treated the same way. It will increase the production of (anti-)baryons in the forward region compared to the previous version of EPOS. This may be seen in the number of muons produced in air shower simulations.

Furthermore, to take into account the property of different jet types, the string tension use for the string fragmentation depends now on the initial partons. Jets coming from quarks or from gluons will not produce the same ratio of (anti-)baryons or strange particles over pions, and it will change the energy evolution of such ratios.

Insert PSN Here

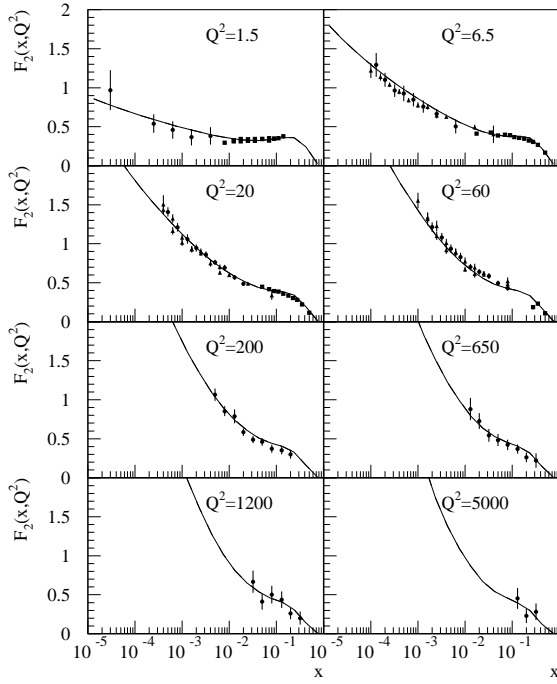


Figure 5: The structure function  $F_2$  for different values of  $Q^2$  together with experimental data from H1 [13], ZEUS [14] and NMC [15].

#### 4. PRELIMINARY RESULTS AT LHC AND OUTLOOK

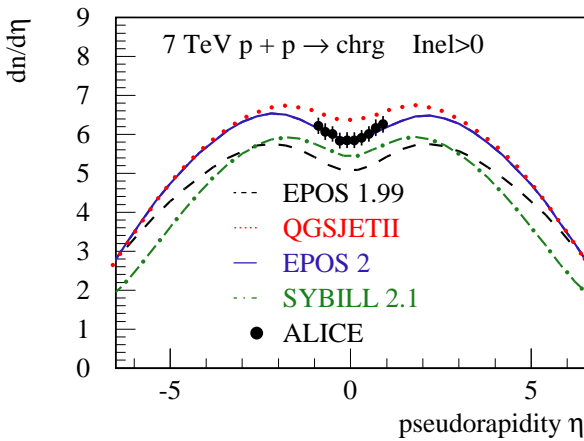


Figure 6: Pseudorapidity distribution in  $pp$  scattering at 7 TeV (INEL>0 trigger), compared to ALICE data (points) for different models : results from EPOS 2 (full) together with results from EPOS 1.99 (dashed), QGSJETII (dotted) and Sibyll 2.1 (dashed-dotted).

The new treatment of the diffraction together with the better calculation of the structure function and the more accurate treatment of the hydrodynamical phase, provide much better results in comparison with LHC data than with EPOS 1.99. We show the pseudo-rapidity distribution at 7 TeV on fig. 6 as an example. EPOS 2 results are compared to EPOS 1.99 and other models used for air shower simulations QGSJETII and Sibyll 2.1 [16] and ALICE data [17].

More detailed results can be found in [18, 19], especially concerning the effect of the hydrodynamical evolution on correlations between secondary particles (Bose-Einstein correlation, ridge).

For the moment EPOS 2 can only be used for minimum bias physics, but in the future it will be possible to select special class of hard events to study specific channels and underlying events [20].

#### References

- 1 R. Bellwied. *Acta Phys. Hung.*, A27:201–204, 2006.
- 2 KASCADE and Pierre Auger Collaboration private communications.
- 3 T. Pierog and K. Werner. *Phys. Rev. Lett.* 101:171101 2008.
- 4 H. J. Drescher et al. *Phys. Rept.*, 350:93–289, 2001.
- 5 F. M. Liu et al. *Phys. Rev.*, D67:034011, 2003.
- 6 M. Bleicher et al. *Phys. Rev. Lett.*, 88:202501, 2002.
- 7 M. Hladik et al. *Phys. Rev. Lett.*, 86:3506–3509, 2001.
- 8 K. Werner et al. *Phys. Rev.*, C74:044902, 2006.
- 9 K. Werner. *Phys. Rev. Lett.*, 98:152301, 2007.
- 10 D. S. Barton et al. *Phys. Rev.*, D27:2580, 1983.
- 11 S. Ostapchenko. *Phys. Rev.*, D74:014026, 2006.
- 12 K. Werner et al., *Phys. Rev. C*83:044904,2010.
- 13 H1 collaboration, Aid et al., *preprint DESY* 96-039,1996.
- 14 ZEUS, M. Derrick et al., *Z.Phys.* C72:399,1996.
- 15 NMC collaboration, Arneodo et al., *Phys. Lett.* B364:107,1995.
- 16 R. Engel, T. K. Gaisser, P. Lipari, and T. Stanev, *Proceedings of 26th ICRC* (Salt Lake City) vol. 1, p. 415, 1999.
- 17 ALICE collaboration, DURHAM database for *Eur.Phys.J.*C68:345-354,2010.
- 18 K. Werner et al., arXiv:1010.0400, *submitted to Phys.Rev. C*, 2010.
- 19 K. Werner et al., arXiv:1011.0375, *submitted to Phys.Rev.Lett.*, 2010.
- 20 S. Porteboeuf, K. Werner, *Eur. Phys. J. C*62:145-150, 2009.